

# Study of Toe Joints to Enhance Locomotion of Humanoid Robots

Shlok Agarwal<sup>1,2</sup> and Marko Popovic<sup>1,2,3,4</sup>

<sup>1</sup>Robotics Engineering Program, <sup>2</sup>Popovic Labs, <sup>3</sup>Physics Department, and <sup>4</sup>Biomedical Engineering Department,  
Worcester Polytechnic Institute

**Abstract**—Most humanoid robots still walk with bent knees and flat feet which is considered highly unnatural, i.e. not biologically inspired, and also energy inefficient. The paradigm and benefits of walking with non-bent knees and with an active toe joint are explored in this study. Non-bent knee walking trajectories are created using an instantaneous capture point (ICP) planner within a momentum based quadratic program (QP) whole body control framework. The toe joint trajectories are obtained as an emergent behavior of the QP determined by under-constraining the objective function and modeling movement of the toe joint as a torsional spring. A comparison between similar systems with and without toe joints reveal a stronger thrust vector during toe-off, reduced knee joint angles and a more human like gait. Experiments in simulation are conducted on the Atlas humanoid robot.

**Keywords:** Humanoid Robots, Toe Joint, Non-bent knees.

## I. INTRODUCTION

Humans are an important source of inspiration for design and development of humanoid robots. The human foot is a complex part of the body with each foot having about 25 % of the total number of bones with large number of ligaments, tendons and muscles. The biological foot architecture and its interaction with the ground reaction forces plays a key role in balance, propelling body motion and shock absorption. The toe region of the foot bears pressure and remains in contact with the ground for about three quarters of the stance phase [1] and is responsible to inject energy in the system during toe-off.

Most humanoid robots have simple flat [2] [3] or curved feet [4] and can benefit from the addition of a toe joint in the foot. For example, on the expense of an extra joint in the leg kinematic chain, the robot can walk faster and climb higher steps [5]. The toe joint extends the length of the stance leg while walking allowing the robot to walk larger steps with non-bent knees. Walking with non-bent knees, i.e. knees that are not unnaturally bent throughout the entire gait cycle, may reduce the torque about the knee and may create a more energy efficient gait somewhat similar to passive dynamic walkers with knees [6].

Heel lift-off during terminal stance reduces joint loading [7]. Having an active toe joint in the stance foot while performing a heel lift-off changes the pitch axis from the un-actuated tip-toe to the actuated toe joint axis, which changes the system configuration to being actuated. Performing a heel

rise during toe-off for flat feet systems results in a line or point contact with the ground but for system with toe joints, there is a surface contact between the toe link and ground during this phase. The surface contact increases the effective area of support polygon increasing controllability during toe-off phase.

Several studies addressed toe joint in the context of humanoid robot locomotion. For example H6 humanoid robot equipped with an active toe joint was able to walk faster, climb higher steps, and even perform extreme actions with its knees in contact with the ground [5] by utilizing ZMP [8] control concepts. A number of feet with passive toe joints [9] [10] [11] [12] were designed for WABIAN-2 which showed stretched knee heel-to-toe human like walking. Using ZMP control, pattern generation and predetermining knee angles, the toe joint was able to provide stronger thrust during toe-off. Petman [13] used a compliant prosthetic foot and principles of ICP [14] for balance to exhibit fast natural human like gait. In another study [15] with Lola robot the active toe joint was used to perform heel-rise during terminal stance to reduce joint loading and augment agility by using the kinematic redundancy. Two torsional springs as toe joints in each foot were utilized to simulate a running gait by predicting the ZMP trajectory and calculating corresponding center of mass (CoM) trajectories in [16]. Here, in difference we do not predetermine the trajectories of the toe joint and allow the optimization based framework and natural dynamics to determine the motion.

In this study, an instantaneous capture point (ICP) planner within a whole body momentum control framework [17] was utilized to evaluate gait performance of a system with toe joint and compare results with a system having flat feet. To simulate a more natural walking gait, the non-bent or 'straight leg' walking framework [18] has been used. The toe joint trajectories are not predetermined and evolve from under-constraining the quadratic program (QP) and modeling the motion of the toe joint as a torsional spring. This approach allows the natural dynamics to govern the motion of the toe joint.

The main contributions of this study include creating a foot model for the Atlas humanoid robot inspired by biomechanical data, modifying ICP control policy and walking state machine to facilitate stable toe joint based walking on flat surfaces and evaluating gait performance with the added joint in the system for Atlas. All the experiments are conducted in the IHMC Open Robotics Software [19] using Simulation Construction Set (SCS) physics based simulator.

S. Agarwal is with the Worcester Polytechnic Institute, Worcester, MA 01609 USA (phone: 508-410-0331; e-mail: ssagarwal@wpi.edu)

M. Popovic is with the Worcester Polytechnic Institute, Worcester, MA 01609 USA (corresponding author, phone: 617-470-8198; fax: 508-831-5886; e-mail: mpopovic@wpi.edu).

The paper is organized as follows. Section II describes the system design. Section III gives a brief overview about the control policies, whole body control, state machine and toe joint behavior. The experiments, results and performance comparison with conventional flat foot systems are presented in section IV. Section V provides inference and thoughts over the methodology and results. Section VI summarizes this approach and provide several concluding remarks.

## II. SYSTEM DESIGN

The Atlas robot is a full-sized hydraulically actuated humanoid robot with 28 actuated joints - 6 in each arm and each leg, 3 in the torso and 1 in the neck. More details about the robot design and control can be found in [20]. By analyzing bio-mechanical data [21] of foot proportions and relative position of metatarsophalangeal (MTP) joint or toe joint in eight sprinters and eight non-sprinters we found that the toe-link forms approximately 18.4 - 23.4 % of the foot size. Since the robot has a larger form factor than humans, we decided to round up and assign 25 % of the original foot as the toe-link. The total size of the foot remained the same. The range of motion (ROM) for toe revolute joint was approximated to the biomechanical data [22] for MTP joint in humans - 45 degrees for toe flexion and 70 degrees for toe extension.

## III. CONTROL POLICY

### A. ICP Control

The instantaneous capture point (ICP) is a ground reference point onto which the robot, thought of as a mathematical inverted pendulum with constant length, has to step to come to an unstable upright equilibrium [14]. It can be introduced as a state transformation of the center of mass (CoM) defined as

$$\xi = \mathbf{x}_{\text{CoM}} + \frac{\dot{\mathbf{x}}_{\text{CoM}}}{\omega} \quad (1)$$

where  $\xi = [\xi_x, \xi_y]$  is the expression used to represent ICP,  $\mathbf{x}_{\text{CoM}} = [x_{\text{CoM}}, y_{\text{CoM}}]$  is the CoM and natural frequency  $\omega = \sqrt{g/z_{\text{CoM}}}$ .

By reordering terms in equation 1, one gets stable first order open loop dynamics between ICP and CoM.

$$\dot{\mathbf{x}}_{\text{CoM}} = -\omega(\mathbf{x}_{\text{CoM}} - \xi) \quad (2)$$

From [17], we get a relation between ICP and Centroidal Momentum Point (CMP) which is another ground reference point that encapsulates the foot's ground reaction force and angular momentum rate [23].

$$\dot{\xi} = \omega(\xi - \mathbf{r}_{\text{CMP}}) \quad (3)$$

where  $\mathbf{r}_{\text{CMP}} = [r_{\text{CMP}x}, r_{\text{CMP}y}]$  is the CMP.

Equation 3 shows unstable first order open loop dynamics. Thus, the CoM dynamics can be split into a stable and unstable part. Since the CoM inherently converges to the ICP over time, the control law is formulated on the CMP [24] which is used to calculate the ICP trajectory. Similar control law formulations can be found in [25].

### B. CMP Way-point Placement

The Zero Moment Point (ZMP) [8] has been widely used to maintain balance of humanoid robots. The ZMP is restricted to only lie in the support polygon whereas the CMP can exist outside as well. As discussed originally in [23] and subsequently revisited in [17] by reducing CMP distance from ZMP, e.g. by maintaining the CMP in the support polygon may reduce the angular momentum rate while walking. The control law is formulated over the CMP reference trajectory and is used to calculate the ICP trajectory as discussed in section III-A. Figure 1 shows the placement of way-points of the CMP on the upcoming footholds.

Each foothold has two CMP way-points with an option to add more points for a more refined control. The CMP trajectory is planned ahead of time for four steps. The force torque sensor which is initially used to compute the CMP of the entire foot now excludes the toe link from the calculation. The first CMP (blue) is placed at the geometric center of the sole and the second (green) is placed at the center of toe joint axis. To guarantee feasibility of trajectories, the trajectories are made smooth using [24].

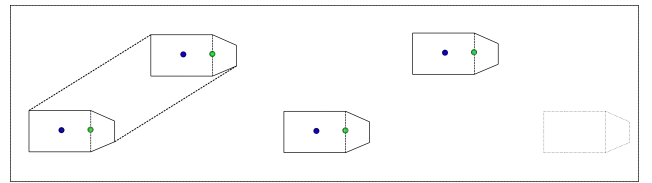


Fig. 1: Figure shows the CMP way-point placement. The blue way point on the foot also referred as the *EntryCMP* is placed between the sole of the foot excluding the toe link. The green way-point also referred as *ExitCMP* is placed at the axis of the toe joint. Both waypoints are aligned with the center line of the foot.

### C. Momentum Based Control

A momentum based control framework coupled with an inverse dynamics solver as described in [17] is used to realize the torque control scheme. A Quadratic Program (QP) solver computes for minimum joint accelerations and force wrenches between the robot and environment at every control step. QP formulation is as follows:

$$\begin{aligned} & \underset{\dot{\mathbf{v}}_d, \rho}{\text{minimize}} && \mathbf{J}_{\dot{\mathbf{h}}_d} + \mathbf{J}_\rho + \mathbf{J}_{\dot{\mathbf{v}}_d} \\ & \text{subject to} && \mathbf{A}\dot{\mathbf{v}}_d + \dot{\mathbf{A}}\mathbf{v} = \mathbf{Q}\rho + \mathbf{W}_g + \sum_i \mathbf{W}_{\text{ext},i} \\ & && \rho \geq 0 \\ & && \mathbf{J}\dot{\mathbf{v}}_d = \mathbf{p} \end{aligned}$$

where  $\mathbf{J}_{\dot{\mathbf{h}}_d} = (\mathbf{A}\dot{\mathbf{v}}_d - \mathbf{b})^T \mathbf{W}_{\dot{\mathbf{h}}_d} (\mathbf{A}\dot{\mathbf{v}}_d - \mathbf{b})$  is the momentum rate objective,  $\mathbf{J}_\rho = \rho^T \mathbf{W}_\rho \rho$  is the contact force regularization and  $\mathbf{J}_{\dot{\mathbf{v}}_d} = \dot{\mathbf{v}}_d^T \mathbf{W}_{\dot{\mathbf{v}}_d} \dot{\mathbf{v}}_d$  is the acceleration regularization.

Here,

- $\dot{\mathbf{v}}_d$  are the desired joint accelerations,  $\rho$  is the basis vector multiplier for contact forces.

- $\mathbf{A}$  is the centroidal momentum matrix,  $\mathbf{b} = \dot{\mathbf{h}}_d - \dot{\mathbf{A}}\mathbf{v}$ ,  $\dot{\mathbf{h}}_d$  is the desired rate of change of centroidal momentum and  $\mathbf{v}$  is the joint velocities matrix.
- $\mathbf{W}_g$  is the wrench due to gravity and  $\mathbf{W}_{\text{ext},i}$  are the external wrenches acting on the robot.
- $\mathbf{Q}$  transforms wrenches from local task frame to the centroidal frame.
- $\mathbf{W}_h$ ,  $\mathbf{W}_p$  and  $\mathbf{W}_{v_d}$  are cost function weighting matrices.
- Motion tasks are concatenated in a matrix form and applied as a constraint to the QP in the format where  $\mathbf{J} = (\mathbf{J}_1^T \cdots \mathbf{J}_n^T)$  could be a geometric jacobian or simple selection matrix based on nature of motion task. Similarly value of  $\mathbf{p} = (\mathbf{p}_1^T \cdots \mathbf{p}_n^T)$  is task dependent.

Based on [17], the motion task for a point or spatial acceleration task for a desired twist can be specified as

$$\mathbf{p}_i = \dot{\mathbf{T}} - \dot{\mathbf{J}}\mathbf{v} \quad (4)$$

where the twist matrix expressed in body frame is  $\mathbf{T} = \begin{pmatrix} \omega \\ \mathbf{v} \end{pmatrix} \in \mathbb{R}^6$  and  $\omega, \mathbf{v}$  are the angular and linear velocity components.

Redundant systems like humanoid robots often need to achieve multiple objectives at the same time like reaching a point in 6D space and simultaneously maintaining balance. Using this momentum control framework, we exploit this redundancy by under-constraining certain motion objectives of the QP to achieve emergent behaviours in the robot. An emergent behaviour is an unplanned behaviour which emerges out of natural dynamics and potentially benefits the movement of the robot. During unforeseen scenarios, having predetermined trajectories may degrade performance. On the other hand, having behaviors which are independent of trajectories might help the robot adapt to the environment. We address this in further detail in section III-E.

#### D. Walking Control

Most humanoid robots walk with bent knees throughout the entire gait which is highly unnatural and energy inefficient. To simulate a more human like walking gait using toe joints, the framework of 'straight leg walking' presented in [18] has been utilized. That framework uses ICP control in a QP momentum control framework and avoids complex CoM height planning.

Non-bent knee walking, i.e. 'straight leg walking' [18], refers to a more natural human like gait with alternating slightly bent and non-bent knees. Having such knee configurations raises the height of the center of mass(CoM), reduces knee torque and increases ground clearance while walking.

1) *Null Space Projection*: The swing and stance leg trajectories are calculated based on ICP control and are set as QP objectives. The vertical momentum objective (as discussed in section III-C) is left unconstrained and height is controlled by biasing leg joint angles in the null space of QP objectives.

To project a desired joint angle in the null space of QP, it is converted to a joint acceleration command using feedback control law:

$$\dot{\mathbf{v}}_d = \mathbf{K}_p(\mathbf{q}_d - \mathbf{q}) + \mathbf{K}_d\mathbf{v} \quad (5)$$

where  $\dot{\mathbf{v}}_d$  is the desired joint acceleration,  $\mathbf{q}_d$  is the desired joint angle,  $\mathbf{q}$  is the current joint angle,  $\mathbf{K}_p$  and  $\mathbf{K}_d$  are proportional and derivative gains.

The desired acceleration is appended as a QP objective in the form [18]:

$$\mathbf{J}_d = (\mathbf{I} - \mathbf{J}_{\text{total}}^+ \mathbf{J}_{\text{total}}) \dot{\mathbf{v}}_d \quad (6)$$

where the  $\mathbf{J}_{\text{total}}$  is the total concatenated jacobian of the robot and  $(\cdot)^+$  is a pseudo operator.

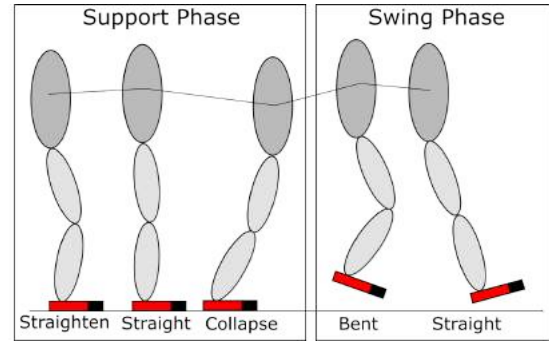


Fig. 2: Walking state machine for the leg during the gait.

2) *State Machine*: A state machine architecture is used to determine null space objectives. The cyclic walking gait is composed of successive support and swing phases which can be formulated as a deterministic state machine with a fixed sequence. Leg configuration in each of these states for each leg is shown in figure 2. The State machine has four distinct states - *Straighten*, *Collapse*, *Bent* and *Straight*. The state transitions are defined as a function of the swing time and foot ground contact. In each state the knee angle changes from current configuration to desired state configuration.

The *Straighten* and *Bent* state for the stance and swing leg are triggered at heel strike. The swing phase is marked with beginning of *Bent* state. The swing time in our experiments is 0.7 seconds. The transitions between *Straighten* to *Straight*, *Straight* to *Collapse*, *Bent* to *Straight* are time-based and defined at 20%, 50% and 40% of the swing time. The *Collapse* state transitions to *Bent* state at heel strike in double support phase. The *Straighten* differs from *Straight* state in the manner that it can only be triggered on foot touchdown. The desired knee joint angles in *Straighten*, *Straight*, *Collapse*, *Bent* are 0, 0, 0.3 and 1.5 radians. These fraction values and joint angles were used in our experiments and can vary for different robots or gaits. With the defined desired angles of the knee joint in each state, equation 6 converts them into an additional QP objectives.

### E. Toe Joint Behaviour

The toe joint plays a key role in the proposed gait cycle. It is used during terminal stance when the swing foot has reached or is reaching the desired foothold. This occurs between the *Collapse* and *Bent* state in figure 2. Actuating the toe joint at this stage increases reachability of swing leg and raises the height of the CoM which aids in case the next step is at a higher elevation.

There are multiple approaches to plan trajectories and increase utility of the toe joint [16] [11] [9]. In every approach, the toe angle is estimated based on the foot position in the gait and trajectories for toe joint are planned accordingly. In this work, we modelled the movement of the toe joint as a torsional spring with the rest position aligned with the flat foot on the ground. When the joint moves, it exerts a torque in the opposite direction proportional to angle of twist. During terminal stance, we constrain a point (using equation 4) on the joint axis of the toe to have zero linear acceleration, roll and yaw but leave the pitch unconstrained. The point is marked as the yellow star on the ground in figure 3. The pitch angle of the toe is left to be determined by the natural dynamics. To maintain the position, roll and yaw of the point in world frame, the QP finds suitable joint accelerations and force wrenches to support keeping the toe link on the ground and achieve other gait objectives simultaneously. The pitch motion about the toe joint as seen in figure 2 is an emergent behaviour caused by under-constraining the QP objective. A similar approach has been used in [18] to create toe-off motion during terminal stance to push the body forward.

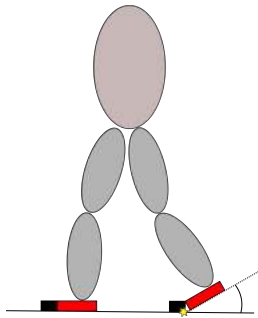


Fig. 3: Toe Pitch during Gait. The linear positions and orientations except the pitch are constrained about the yellow star point during toe-off.

The proposed toe joint behaviour alters the performance of the gait in two aspects. During the toe-off phase, the toe link is the last link in contact with the ground. Right before the link lifts off the ground, there is a torque generated about the toe joint proportional to the pitch angle with respect to the ground. This force on the tip of the toe link creates a strong thrust vector in the direction of movement of leg which helps moving the CoM forward. The second benefit is during double support phase where the leading leg bends the knee to move the CMP towards the polygon created by the leading leg. Instead of bending the knee at this time, the toe joint actuates and pushes the CMP forward and also raises

the height of the CoM. This is illustrated in figure 3 where the toe is making an angle with respect to the ground. Both of these behaviours are achieved by under-constraining the toe pitch angle and generating torque proportional to angle of pitch.

## IV. RESULTS

The algorithm is implemented in the IHMC Open Source Software [19] system and is simulated in the Simulation Construction Set (SCS) simulator. A walking gait for five steps with step length of 0.5 m, swing height of 0.15 m, swing time of 0.70 s and transfer time of 0.25 s starting with the left foot is used to compare performance between straight leg walking presented in [18] without toe (blue) joint and our system with the toe joint (red). Employing the same control framework, model, environment and simulator, we attempt to inspect a more even comparison between both systems and aim to judge clear benefits of having a system with toe joint.

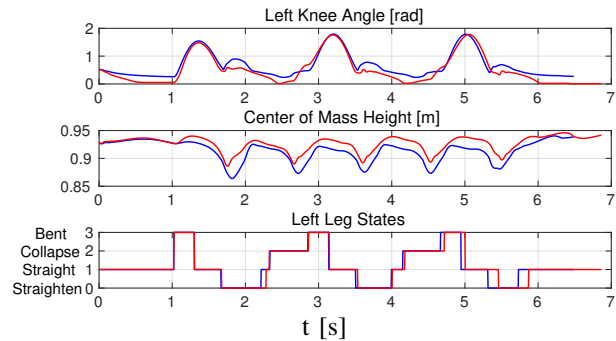


Fig. 4: Knee angle and CoM height trajectory along with state machine transitions. The blue lines represent system with toe joint and red is for system without toe joint.

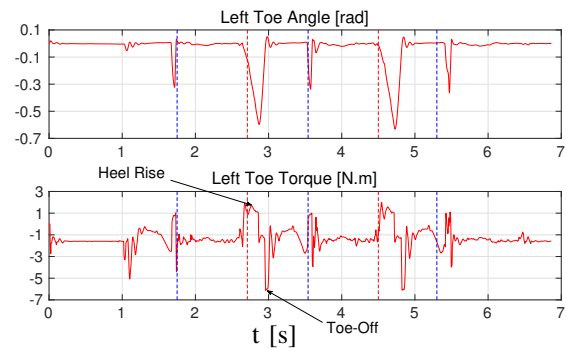


Fig. 5: Angle and torque about the toe joint axis. The heel strike and toe-off are marked with dotted blue and red lines.

Figure 4 shows the knee angle and CoM height along with the state transitions of the left foot for both systems. The *Bent* state marks the beginning of the swing phase with the knee bending to create ground clearance for moving the foot forward. Following the *Bent* state, the state transitions to *Straight* state to reach desired foothold. At touchdown,

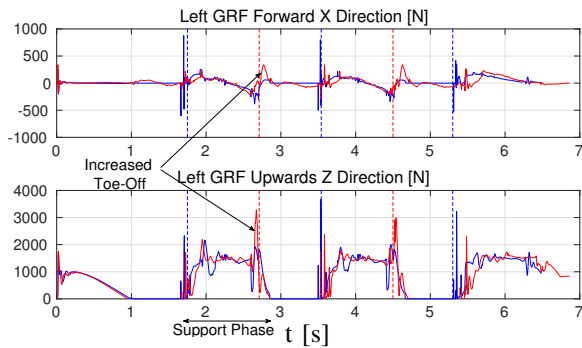


Fig. 6: Ground Reaction Forces for left foot. System with toe joint (red) has stronger toe-off compared to system without toe (blue). The heel strike and toe-off are marked with dotted blue and red lines.

*Straighten* and *Straight* state straighten the knee and maintain torso orientation. The *Collapse* state is triggered late in stance phase to extend reachability of swing leg (addressed in III-E). The left foot takes three steps and each step is characterized by two peaks in the knee joint angle.

Figure 5 shows the angle and torque about the toe joint during the gait. The heel strike and toe-off are marked with dotted blue and red lines. The toe joint motion is governed by body link motions, inertia and optimization constraints. During heel strike, the toe joint moves slightly due to foot inertia and during toe-off, the toe joint rises and then pushes on the ground. Figure 6 shows the GRF in the forward and upwards direction for the left foot highlighting heel strike, support and toe-off forces. The gait profile of a single step can be seen in figure 7.

## V. DISCUSSION

The first peak in figure 4 demonstrates the knee bending in order to create ground clearance for the swing leg. Our interest lies in the second peak which is the phase where the swing leg has touched down and the robot is in double support phase. To move the CMP forward for maintaining stability in the next step, our system (red) extends the stance leg length by actuating the toe which provides two key benefits. It reduces the knee angle (second peak) and it also decreases the vertical deviations of the CoM. If we assume the CoM trajectory to be similar to an inverted pendulum [26], the toe joint is actuated early when CoM is falling and it increases the height. This keeps the CoM in our system (red) higher throughout the gait.

The movement of the toe joint is an emergent behavior out of the whole body optimization addressed in section III-E. As seen in figure 5, before toe-off there is a heel-rise phase where the stance leg length is extended to raise the body. This corresponds to the downward peak in the toe joint angle. Due to the angle deflection, a torque is applied in the opposite direction to correct the angle. This motion leads to the toe pushing on the ground providing additional thrust in the sagittal plane.

The ground reaction forces (GRF) for human walking as observed in [27] shows two peaks with one being at heel strike and one at toe-off with the later being larger indicating a strong push forward when the foot leaves the ground. For our system (red), we observe an increased toe-off with higher force magnitude in the X (forward) and Z (upwards) direction resulting in an increased force magnitude. This closely matches the GRF for human walking.

## VI. CONCLUSIONS

In this paper, the use of active toe joint to enhance locomotion capabilities of humanoid robots is explored. An ICP planner within a momentum control QP framework is used to generate walking trajectories. The trajectories of the toe joint are an emergent behavior of the QP. They are determined by under-constraining the QP objective and further modeling torque control based on torsional spring model. During toe-off phase, the compliance of the joint allows the toe link to rotate and when the foot is about to leave the ground, the link injects energy in the system. Using this framework, Atlas was able to achieve a more natural, dynamically balanced walking gait without knees substantially bent throughout the entire gait cycle in simulation. The GRF profile also appears more human like in sense that it shows an increase trust during toe-off. With the supporting results for knee joint angles, CoM height and GRF, this control approach for a system with active toe joints help us take a step towards human like walking for humanoid robots.

## VII. FUTURE WORK

The ability to create a stronger thrust vector during toe-off could augment existing controllers to walk faster with and more efficiently. More experiments can help evaluate agility and energy efficiency due to addition of toe joint in the system. Preliminary energy calculations using torque and angular velocity information from the simulator revealed an improved efficiency in the sagittal plane. Hardware implementation with more rigorous experiments would be reported in the forthcoming works.

## ACKNOWLEDGMENT

We would like to thank Professor Mike Gennert and members of the WPI Humanoid Robotics Lab for their insights and discussion.

## REFERENCES

- [1] J. Hughes, P. Clark, and L. Klenerman, "The importance of the toes in walking," *Bone & Joint Journal*, vol. 72, no. 2, pp. 245–251, 1990.
- [2] G. Metta, G. Sandini, D. Vernon, L. Natale, and F. Nori, "The icub humanoid robot: an open platform for research in embodied cognition," in *Proceedings of the 8th workshop on performance metrics for intelligent systems*. ACM, 2008, pp. 50–56.
- [3] N. A. Radford, P. Strawser, K. Hambuchen, J. S. Mehling, W. K. Verdeyen, A. S. Donnan, J. Holley, J. Sanchez, V. Nguyen, L. Bridgewater, et al., "Valkyrie: Nasa's first bipedal humanoid robot," *Journal of Field Robotics*, vol. 32, no. 3, pp. 397–419, 2015.
- [4] K. Yamane and L. Trutoiu, "Effect of foot shape on locomotion of active biped robots," in *Humanoid Robots, 2009. Humanoids 2009. 9th IEEE-RAS International Conference on*. IEEE, 2009, pp. 230–236.

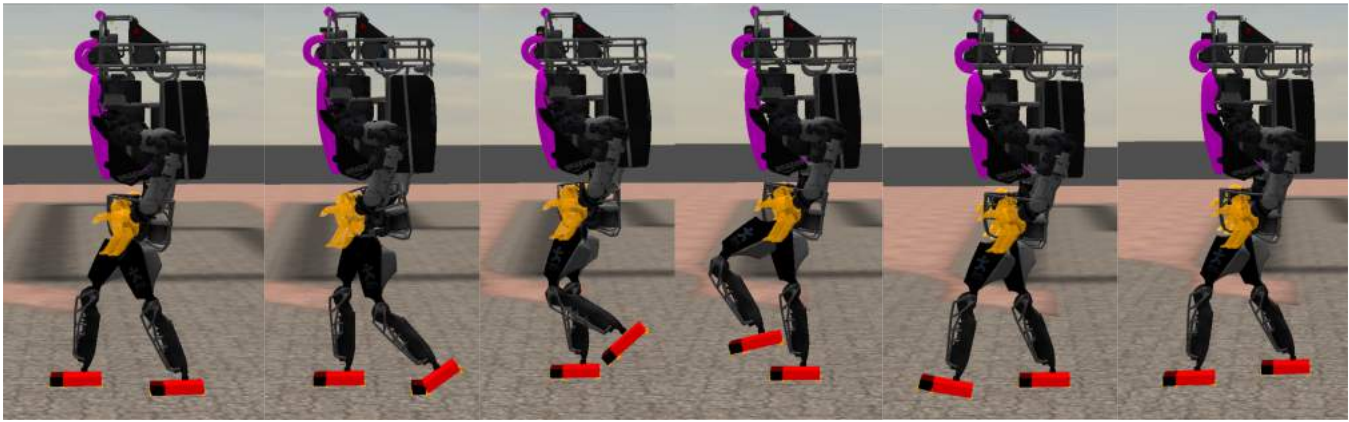


Fig. 7: Gait profile of single step for Atlas robot

- [5] K. Nishiwaki, S. Kagami, Y. Kuniyoshi, M. Inaba, and H. Inoue, "Toe joints that enhance bipedal and fullbody motion of humanoid robots," in *Robotics and Automation, 2002. Proceedings. ICRA'02. IEEE International Conference on*, vol. 3. IEEE, 2002, pp. 3105–3110.
- [6] T. McGeer, "Passive walking with knees," in *Robotics and Automation, 1990. Proceedings., 1990 IEEE International Conference on*. IEEE, 1990, pp. 1640–1645.
- [7] D. C. Kerrigan, U. Della Croce, M. Marciello, and P. O. Riley, "A refined view of the determinants of gait: significance of heel rise," *Archives of physical medicine and rehabilitation*, vol. 81, no. 8, pp. 1077–1080, 2000.
- [8] M. Vukobratović and B. Borovac, "Zero-moment point—thirty five years of its life," *International journal of humanoid robotics*, vol. 1, no. 01, pp. 157–173, 2004.
- [9] Y. Ogura, K. Shimomura, H. Kondo, A. Morishima, T. Okubo, S. Momoki, H.-o. Lim, and A. Takanishi, "Human-like walking with knee stretched, heel-contact and toe-off motion by a humanoid robot," in *Intelligent Robots and Systems, 2006 IEEE/RSJ International Conference on*. IEEE, 2006, pp. 3976–3981.
- [10] K. Hashimoto, Y. Takezaki, K. Hattori, H. Kondo, T. Takashima, H.-o. Lim, and A. Takanishi, "A study of function of foot's medial longitudinal arch using biped humanoid robot," in *Intelligent Robots and Systems (IROS), 2010 IEEE/RSJ International Conference on*. IEEE, 2010, pp. 2206–2211.
- [11] P. Kryczka, K. Hashimoto, H. Kondo, A. Omer, H.-o. Lim, and A. Takanishi, "Stretched knee walking with novel inverse kinematics for humanoid robots," in *Intelligent Robots and Systems (IROS), 2011 IEEE/RSJ International Conference on*. IEEE, 2011, pp. 3221–3226.
- [12] K. Hashimoto, H. Motohashi, T. Takashima, H.-o. Lim, and A. Takanishi, "Shoes-wearable foot mechanism mimicking characteristics of human's foot arch and skin," in *Robotics and Automation (ICRA), 2013 IEEE International Conference on*. IEEE, 2013, pp. 686–691.
- [13] G. Nelson, A. Saunders, N. Neville, B. Swilling, J. Bondaryk, D. Billings, C. Lee, R. Playter, and M. Raibert, "Petman: A humanoid robot for testing chemical protective clothing," *Journal of the Robotics Society of Japan*, vol. 30, no. 4, pp. 372–377, 2012.
- [14] J. Pratt, J. Carff, S. Drakunov, and A. Goswami, "Capture point: A step toward humanoid push recovery," in *Humanoid Robots, 2006 6th IEEE-RAS International Conference on*. IEEE, 2006, pp. 200–207.
- [15] S. Lohmeier, T. Buschmann, and H. Ulbrich, "Humanoid robot lola," in *Robotics and Automation, 2009. ICRA'09. IEEE International Conference on*. IEEE, 2009, pp. 775–780.
- [16] S. Kajita, K. Kaneko, M. Morisawa, S. Nakaoka, and H. Hirukawa, "Zmp-based biped running enhanced by toe springs," in *Robotics and Automation, 2007 IEEE International Conference on*. IEEE, 2007, pp. 3963–3969.
- [17] T. Koolen, S. Bertrand, G. Thomas, T. De Boer, T. Wu, J. Smith, J. Engelsberger, and J. Pratt, "Design of a momentum-based control framework and application to the humanoid robot atlas," *International Journal of Humanoid Robotics*, vol. 13, no. 01, p. 1650007, 2016.
- [18] R. J. Griffin, G. Wiedebach, S. Bertrand, A. Leonessa, and J. Pratt, "Straight-leg walking through underconstrained whole-body control," *arXiv preprint arXiv:1709.03660*, 2017.
- [19] Sylvain Bertrand, D. Calvert, J. Pratt, G. Wiedebach, R. Griffin, btshrewsbury, J. Smith, T. Koolen, N. Mertins, D. Stephen, S. McCrory, neyssette, mahopkins, cmschmid, jcarff, K. Cesare, aprvs, egalbally, mj fl, P. Abeles, edilee, pneuhaus, A. B. Filho, W. Rifenburg, N. Choe, K. PetrÁánek, stespenc83, OlgerSiebinga, S. Agarwal, and lbunch, "ihmrobotics/ihmc-open-robotics-software: 0.11 Release Notes," Jan. 2018. [Online]. Available: <https://doi.org/10.5281/zenodo.1135300>
- [20] S. Kuindersma, R. Deits, M. Fallon, A. Valenzuela, H. Dai, F. Permenter, T. Koolen, P. Marion, and R. Tedrake, "Optimization-based locomotion planning, estimation, and control design for the atlas humanoid robot," *Autonomous Robots*, vol. 40, no. 3, pp. 429–455, 2016.
- [21] J. R. Baxter, T. A. Novack, H. Van Werkhoven, D. R. Pennell, and S. J. Piazza, "Ankle joint mechanics and foot proportions differ between human sprinters and non-sprinters," *Proceedings of the Royal Society of London B: Biological Sciences*, vol. 279, no. 1735, pp. 2018–2024, 2012.
- [22] O. Rasmussen, "Stability of the ankle joint: analysis of the function and traumatology of the ankle ligaments," *Acta Orthopaedica Scandinavica*, vol. 56, no. sup211, pp. 1–75, 1985.
- [23] M. B. Popovic, A. Goswami, and H. Herr, "Ground reference points in legged locomotion: Definitions, biological trajectories and control implications," *The International Journal of Robotics Research*, vol. 24, no. 12, pp. 1013–1032, 2005.
- [24] J. Engelsberger, G. Mesesan, and C. Ott, "Smooth trajectory generation and push-recovery based on divergent component of motion," in *Intelligent Robots and Systems (IROS), 2017*.
- [25] J. Engelsberger, C. Ott, M. A. Roa, A. Albu-Schäffer, and G. Hirzinger, "Bipedal walking control based on capture point dynamics," in *Intelligent Robots and Systems (IROS), 2011 IEEE/RSJ International Conference on*. IEEE, 2011, pp. 4420–4427.
- [26] S. Kajita, F. Kanehiro, K. Kaneko, K. Yokoi, and H. Hirukawa, "The 3d linear inverted pendulum mode: A simple modeling for a biped walking pattern generation," in *Intelligent Robots and Systems, 2001. Proceedings. 2001 IEEE/RSJ International Conference on*, vol. 1. IEEE, 2001, pp. 239–246.
- [27] J. Nilsson and A. Thorstensson, "Ground reaction forces at different speeds of human walking and running," *Acta Physiologica*, vol. 136, no. 2, pp. 217–227, 1989.